APPLYING FINITE ELEMENT METHOD FOR WELLBORE STRESS AND STABILITY ANALYSIS

ỨNG DỤNG PHƯƠNG PHÁP PHẦN TỬ HỮU HẠN TRONG PHÂN TÍCH ỨNG SUẤT VÀ ỔN ĐỊNH GIẾNG KHOAN

Do Quang Khanh*, Tran Thi Mai Huong,
Nguyen Thi Thu Trang, Vo Huynh Nhan, Kieu Phuc

Faculty of Geology and Petroleum Engineering,
Ho Chi Minh City University of Technology (HCMUT),
National University – Ho Chi Minh City (VNU-HCM), Vietnam
** dqkhanh@hcmut.edu.vn*

Abstract: *The objectives of study aim to analyse the stress and stability around a wellbore during petroleum activities. Therefore, in this paper the stress and stability analysis of a petroleum wellbore at a depth of 2800 m was carried out using the finite element code ANSYS®. The models were analysed to investigate the effects of the equal and differential far-field stresses around the wellbore. Differential far-field stresses are the main cause of the elliptical deformation of stress trajectories around a wellbore.*

Keywords: *Finite element, stress, stability, wellbore.*

Classification number: *2.1*

Tóm tắt: *Mục tiêu của nghiên cứu nhằm phân tích ứng suất và ổn định xung quanh giếng trong các hoạt động dầu khí. Do vậy, trong bài báo này việc phân tích ứng suất và ổn định của giếng khoan dầu khí ở độ sâu 2800 m đã được thực hiện bằng cách sử dụng mã phần tử hữu hạn ANSYS®. Các mô hình đã được phân tích để khảo sát các ảnh hưởng của các trường ứng suất bằng nhau và khác biệt lên giếng khoan.Các trường ứng suất khác biệt là nguyên nhân chính gây nên sự biến dạng ellip của các quỹ đạo ứng suất xung quanh giếng.*

Từ khóa: *Phần tử hữu hạn,ứng suất, ổn định, giếng khoan.*

Chỉ số phân loại: *2.1*

1. Introduction

Rock in natural state is subjected to the in-situ stresses in three principal directions and magnitudes, including the verical stress and two horizontal stresses. The two horizontal stresses may equal, but in general are differential. When drilling into a formation, the rock around the wellbore is subjected to stresses caused by the material being removed. Drilled wellbore is only subject to fluid pressure in the wellbore causing a change in the state of stress around the wellbore due to the fluid pressure in the wellbore that usually does not match the in-situ stresses [1], [2]. The redistribution of the stress state will affect strongly the wellbore stability. If the redistributed stresses exceed rock strength, rock surrounding the wellbore is deformed and may fail. Two common failure mechanisms around the wellbore are: Tensile failure and compressive failure. Under the compressive failures, the rock caves may spall off, creating breakouts. When the compressive hoop stress around a hole can be large enough to exceed the rock compressive strength, the rock around the wellbore fails and stress-inducedwellbore breakouts form [3], [4].

The main objectives of this study are to aim the stress and stability analyse for a wellbore during petroleum activities using finite element method and the concepts of porouselasticity theory. They include:

- Building a finite element model (FEM) for a petroleum wellbore at a depthof 2800 m surrounded by the far-field stresses along with the pore pressure;

- Investigating the effects of the equal and differential far-field stresses around a wellbore to the wellbore stress and stability analyse.

2. Modeling by finite element method

The finite element method is used tocompute the stress trajectories and contours around a circular wellbore drilled into the homogeneous rock formation. The studied region is divided into a number of finite elementsconnected by nodal points. Each node and element must be numbered, and the coordinate location of each node linked with each element must be input to the model. These elements are described by differential equations and solved through mathematical models. The main advantage of the FEM is to permit the computation and analyse for materials with the different properies and behaviours under the different load conditions in anisotropic medium [5]. In general, in order to build a finite numerical model, it is necessary to specify three fundamental components for the calculations: Element finite mesh; Constitutive model and material properties; and Initial conditions and boundary conditions. Finite element numerical models are generated by using the finite element code of finite element software package ANSYS.The ANSYS software represents the Von Misesstress as equivalent stress magnitude. Magnitudes of Von Mises stress also are calculated from the principal stresses for the contour plots of these numerical models [6].

In this paper, the horizontal section of a circular wellbore is considered at a depth of 2800 m with the verical stress Sv calculated by using the vertical stress gradient of 22 MPa/km from well log data.

Boundary constraints will represent a key element in understanding the modeling results. These include equal far-field stresses ($S_H = S_h = 0.7S_V$ = 44MPa) or differential far-field stresses ($S_H = S_V$ = 62MPa and $S_h = 0.7S_V$ = 44MPa) (as shown inFigure 1) at the model boundary and the drilling mud pressure of 28MPa applied at the circular wellbore boundary.

Besides, pore pressure of 26.12 MPa at the depth of 2800 m is estimated from hydrostatic pressure gradient assuming 9.33 MPa/km (equivalent to 0.433 psi/ft). Displacements along x axis and y axis of the model boundaries have been assumed zero values. The finite element modeling is carried out in the horizontal plane.

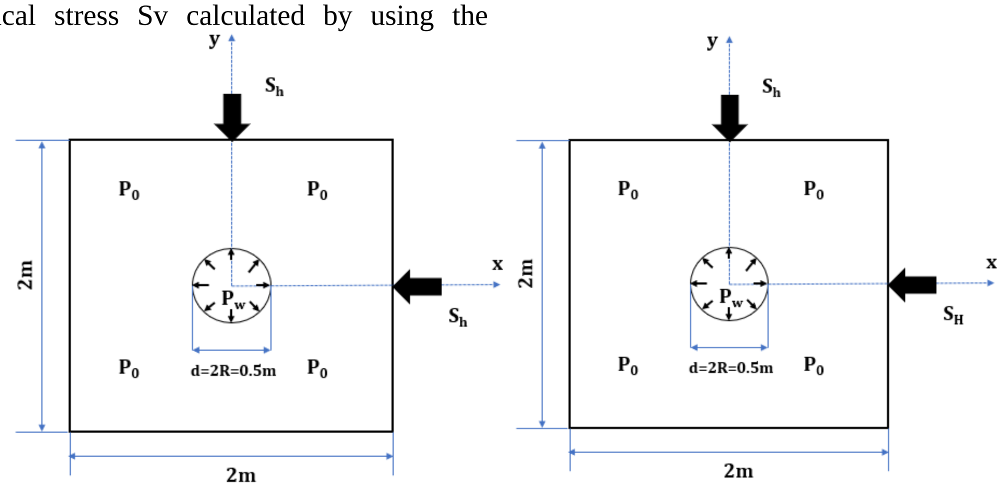

Figure 1. *Models and boundary constraints under: Equal far-field stresses (onthe top) and differential far-field stresses (on the below).*

For numerical modelling of stress around a wellbore, the homogeneous rock mass of 2x2 sq. m area with a centrally located wellbore of diameter 0.5 m has been considered.

Its mechanical rock properties have been assumed for modeling such as Young's modulus of 30 GPa, Poisson's ratio of 0.27. Due to the symmetry, only a quarter sector of this rock mass is modeled with the plane strain elements.

Moreover, in order to the accuracy of results a refined mesh was built along with the above boundary constraints as shown in figure 2.

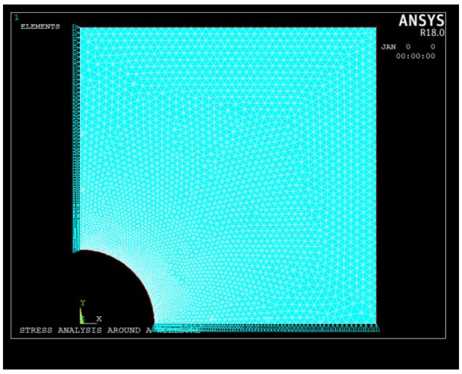

Figure 2. *A refined mesh of only a quarter sector of the considered rock mass.*

3. Results and discussion

The model subjected to equal far-field stresses showed the uniform variation of Von Mises stress ranging from 35.9 MPa at the boundary of rock mass to 69.3 MPa prevailing around the wellbore (figure 3).

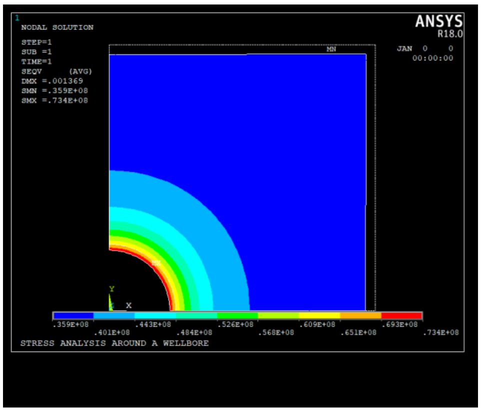

Figure 3. *Von Mises stress contour for the model under equal far-field stresses.*

The stress vector plot displayed the redistribution of horizontal stress direction around the wellbore. However, it also showed the uniform variation of horizontal stress direction from the boundary of rock mass to the wellbore at all sites (figure 4).

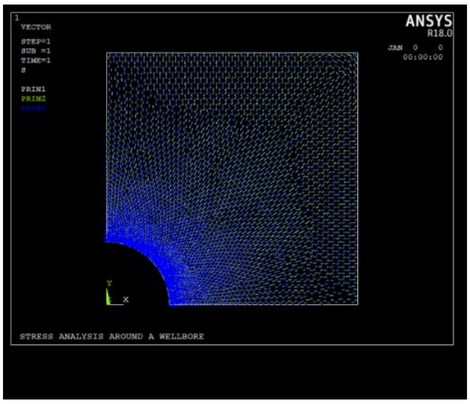

Figure 4. *Stress vector plot for the model under equal far-field stresses.*

Moreover, the resultant displacement contour and displacement vector plot for the model under equal far-field stresses also showed uniform variation along the boundary and the wellbore diameter is reduced at all sides (figure 5).

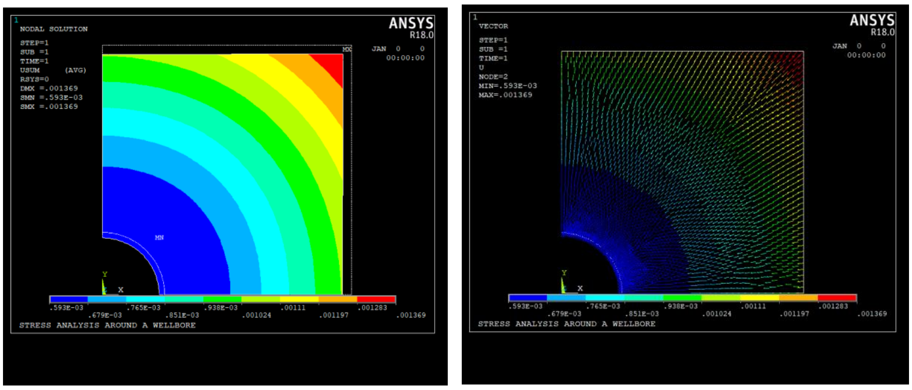

Figure 5. *Displacement contour (on the top) and displacement vector plot (on the below) for the model under equal far-field stresses.*

The next model subjected to differential far-field stresses showed the Von Mises stress contour (figure 6), indicating the stress magnitude of 99.2MPa to 38.7 MPa along the direction of minimum horizontal stress Sh, i.e. the direction of long axis of the elliptical wellbore and is maximum 99.2 MPa at the wall wellbore. However, only the stress magnitude of 8.39 MPa to 38.7 MPa is along the direction of maximum horizontal stress SH, i.e. the direction of short axis of the elliptical wellbore.

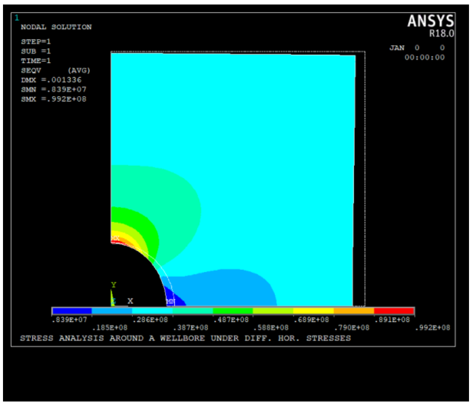

Figure 6. *Von Mises stress contour for the model under differential far-field stresses.*

The stress vector plot (figure 7) also indicated that the minimum horizontal stress vector is rotated towards the long axis of ellipse aligning parallel to the far-field Sh direction. The maximum horizontal stress vector is aligned perpendicular to the Sh direction.

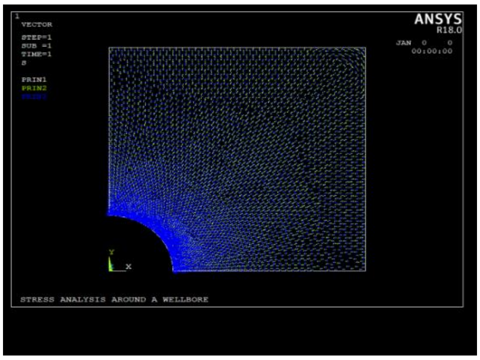

Figure 7. *Stress vector plot for the model under differential far-field stresses.*

Besides, the resultant displacement contour and displacement vector plot for the model under differential compressive horizontal stresses also showed clearly deformation of the wellbore wall (Figure 8). Wellbore becomes elliptical with its long axis oriented towards the Sh direction. Wellbore diameter is increased along the Sh direction and shortened along the SH direction.

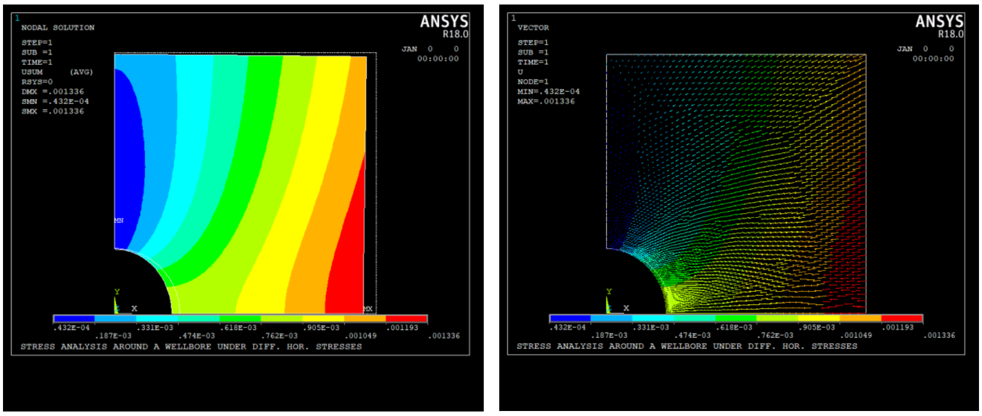

Figure 8. *Displacement contour (on the top) and displacement vector plot (on the below) for the model under differential far-field stresses.*

The redistribution of Von Mises contour for the model under equal far-field stresses (figure 3) and differential far-field stresses (figure 6) is very different. They will affect strongly the wellbore stability. If under equal far-field stresses, the redistributed stresses around the wellbore still do not exceed the rock strength so the wellbore will be stability. However, under differential far-field stresses, the stress concentration around the wellbore appeared along the Sh direction. A region with its redistributed stresses, which overcome the rock strength of 80.0 MPa, will be under the compressive failures. The rock spalling off the wellbore wall due to differential far-field stresses will create breakouts.

These model results can be verified with image logs of any area under the wellbore condition will indicate the Sh direction. They also indicated similar results on the direction and relative extension of observed breakouts from the image logs (figure 9) like Ultrasonic Televiewer and Formation Micro Imager for the wellbores, which were considered by Zoback et al., 2003 [2] as they discussed the wellbore elongation under differential stresses. Breakouts are observed as dark bands (low reflection amplitudes) on opposite sides of the well in Ultrasonic Televiewer Image logs (well A) and out-of-focus zones on Formation Micro Imager logs (well B).

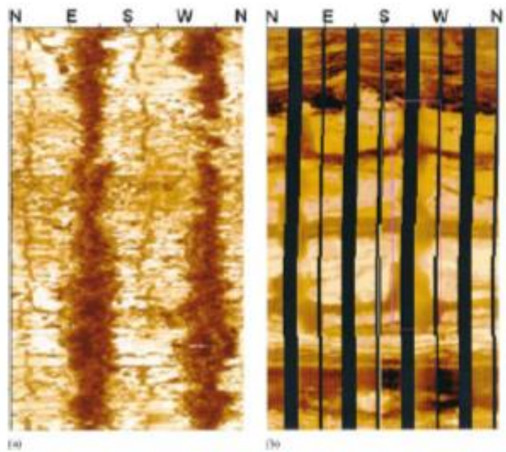

Figure 9. *Illustrations of borehole breakouts in Ultrasonic Televiewer Image logs in well A and Formation Micro Imager logs in well B (after Zoback et al. [2]).*

4. Conclusions

Numerical models applied the finite element method and the concepts of porous elasticity theory to model and analyse the stress redistribution of the rock formation for the wellbore stability.

Numerical models indicated that differential far-field stresses are the main cause of the elliptical deformation of stress trajectories around a wellbore. Modeling results showed the good agreements of the direction and relative extension of the observed breakouts from the image logs of wellbores ❑

Acknowledgement

Authors would like to acknowledge Faculty of Geology and Petroleum Engineering, Ho Chi Minh City University of Technology (HCMUT), Vietnam National University – Ho Chi Minh City (VNU-HCM), Vietnam for their helps and discussions. This research is funded by Ho Chi Minh City University of Technology - VNU-HCM under **grant number T-ĐCDK-2017-92**.

References

[1] Fjær, E., Holt, R. M., Horsrud, P., Raaen, A. M., Risnes, R., (2008), *Petroleum Related Rock Mechanics*, 2nd Edition, Elsevier.

Zoback, M.D., Barton, C.A., Brudy, M., Castillo, D.A., Finkbeiner, T., Grollimund, B.R., Moosb, D.B., Peska, P., Wardb, C.D. and Wiprut, D.J., (2003), *Determination of stress orientation and magnitude in deep wells*, International Journal of Rock Mechanics & Mining Sciences, 40, 1049–1076.

[2] Zoback, M. D., Daniel, M. and Mastin, L., (1985), *Wellbore Breakout and in-situ stress*, Journal of Geophysical Research, 90, 5523-5530.

[3] Khanh, D. Q., (2013), Doctoral Dissertation: *Characterizing the full in-situ stress tensor and its applications for petroleum activities*, Dept. Of Energy and Resources Engineering, Chonnam National University, Korea.

[4] Charrerjee, R. and Mukhopadhyay, M., (2003), *Numerical modelling of stress around a wellbore*, SPE 80489.

[5] ANSYS® Inc. (2017), *ANSYS Manuals, Release 18.2-2017*

Ngày nhận bài: 8/3/2019
Ngày chuyển phản biện: 11/3/2019
Ngày hoàn thành sửa bài: 2/4/2019
Ngày chấp nhận đăng: 9/4/2019